Optimizing Power Delivery in PWM Motor Driver ICs

Thermal Behavior of Single-Phase, Three-Phase Single-Chip PWM Amplifiers SA57-IHZ, SA306-IHZ

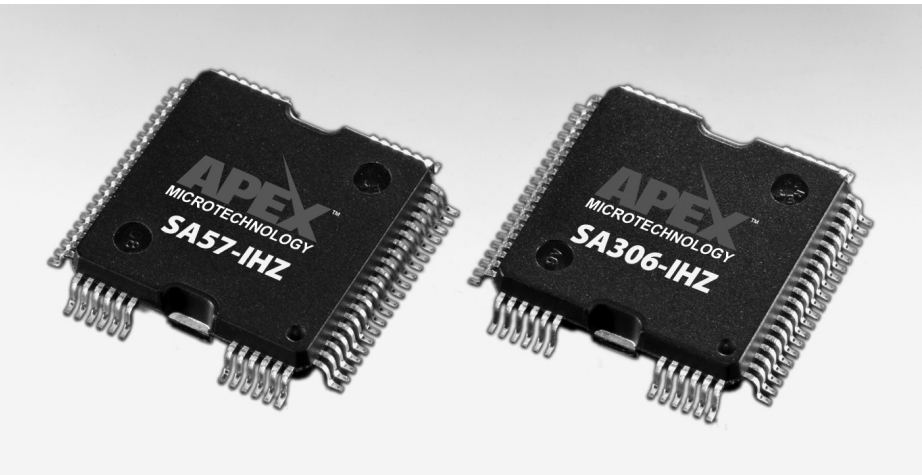

Contents

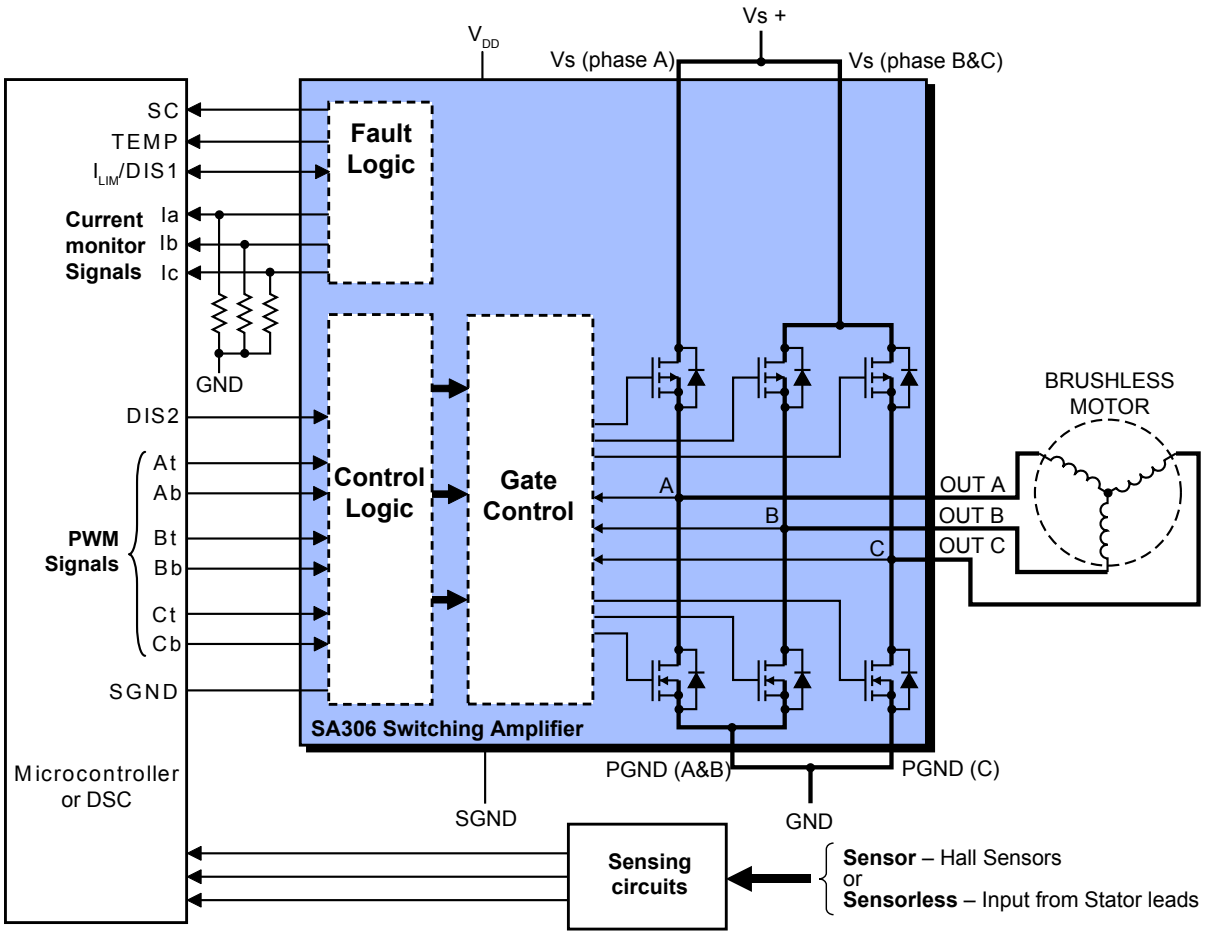

Figure 1. System Block Diagram using the 3-Phase SA306-IHZ Device

Introduction

The Apex SA306-IHZ is an advanced 3-phase single chip amplifier, designed for use as an independent power stage to drive 3-phase brushless DC motors. It incorporates a 3-phase PWM amplifier that accepts six independent control signals. This enables a designer to choose from a wide variety of control signals as appropriate for the commutation method chosen.

This Application Note discusses differences in the thermal behavior of the device relating to mounting techniques, methods of modulation of the power stage and examines some techniques to improve system performance and overall efficiency.

In order to choose the appropriate thermal design for a particular application and for the basic dimensioning of the heatsink, the calculation of the first-order thermal approximation is a good starting point. There are some application specific aspects to be taken into account before starting the basic system design. This Application Note covers some of these basic design steps, data and ideas to carry forward so the design can achieve the best results.

Device Overview

Both the SA306-IHZ and SA57-IHZ devices incorporate all of the sub-systems necessary to drive a brushed or brushless DC motor under the control of an MCU or DSP. At maximum output these devices are capable of safely operating motors approaching 0.5 hp. Like many traditional motor drive products, SA devices integrate control, power supply, gate drive and power stage into a single IC. Unlike competing devices, this series is specifically designed for MCU or DSP control and integrate features that enable implementation of modern commutation techniques, resulting in higher efficiency drive stages. Both SA306-IHZ and SA57-IHZ devices consist of major blocks, as shown in Figure 1. The primary difference between the two devices is the number of phases supported; the SA306-IHZ supports three phases while the SA57-IHZ supports two.

A key feature of this series is the ability to directly control the output FETs. This enables modern commutation schemes such as field-oriented, vector-oriented, and sinusoidal to be implemented within the controller with no in-

tervening circuitry. This architecture simplifies circuit design and reduces EMC/EMI. These devices take the inputs for each gate and provides buffering and drive to the companion FET.

Another significant feature is built-in current sense. Current sense is available for each of the phases from a separate output pin. The output current of the sense pins is ~1/5000th of the phase current. The current sense pins provide direct, real-time feedback to the controller. Current sense is performed at the high-side only. Sensing of low-side currents under braking or flyback conditions is not supported.

Over-temperature, short-circuit and current limit are also implemented. These fault signals provide important feedback to the system controller which can safely disable the output drivers in the event of a fault condition. These topics are discussed in greater detail in Reference 3.

Both the SA306-IHZ and SA57-IHZ implement a cycle-by-cycle current limit scheme. This allows variable user-defined current limit thresholds without damage to the device. However, even in this mode, the user must consider and plan for excessive current excursions which could result in excessive power dissipation.

The architecture of the SA306-IHZ and SA57-IHZ devices enables the designer to configure dynamically-changing current limiting in the device in response to changing system operating conditions. The SA306-IHZ or SA57-IHZ data sheets specify a peak current of 17 amperes. However, if desired the designer can choose to lower this limit or to disable the feature altogether.

In applications where the current in the motor is not directly controlled, both the average current rating of the motor and the inrush current must be considered. For example, a 1 A continuous motor might require a drive amplifier that can deliver well over 10 A PEAK in order to provide the required start-up torque. The cycle-by-cycle current limit feature enables the SA57-IHZ/SA306-IHZ to safely and easily drive a wide range of brush and brushless motors through a startup inrush condition. With limited current, the starting torque and acceleration are also limited. The plots in Figure 2 illustrate starting current and back EMF with and without current limit enabled.

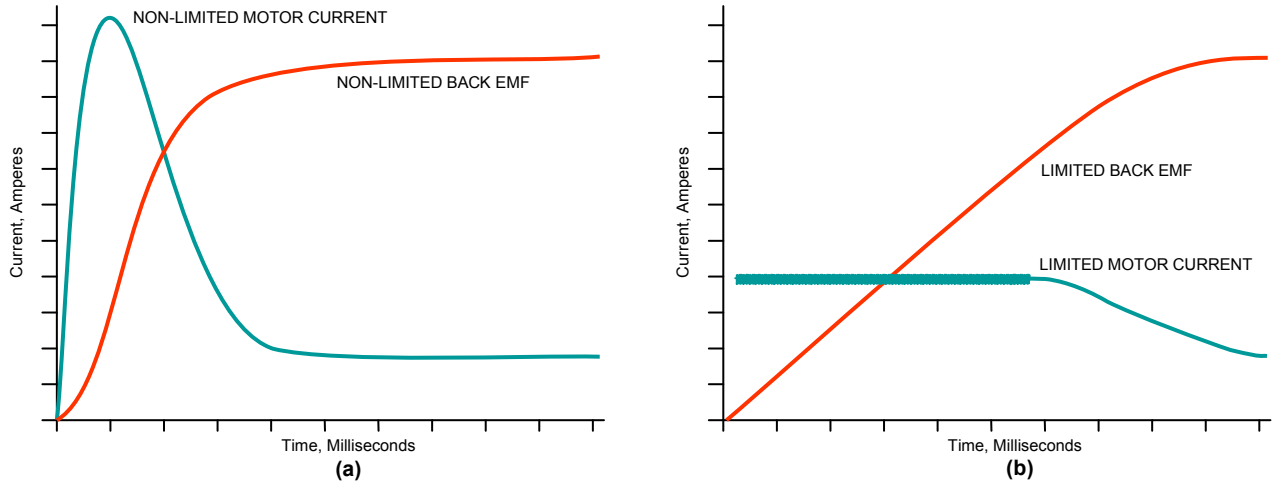

Figure 2. Motor Current Behavior at Startup — (a) Without cycle-by-cycle current limit. (b) With cycle-by-cycle current limit

More information on these and other features of the SA306-IHZ and SA57-IHZ can be found in the product data sheets, as well as any associated Application Notes listed in the Reference section found at the end of this document.

Optimizing Thermal Performance

All power devices, from FETs and IGBTs to large microprocessors, dissipate power in the form of heat. For devices whose primary purpose is power conversion or power transmission appropriate management of heat is the key to determining how much power can be safely processed by the device. This fact applies to specification limits as well. A device may be rated for 5 A continuous but the system designer must always take care that the power lost in the form of heat does not result in damage to the device.

It must be noted that total output power and total power dissipation are dependent on both the output current and operating voltage. For all mounting techniques discussed in this Application Note the effect of voltage and current levels will produce variations in power dissipation. For example, graphs of low power operation show heat dissipation for a given output power. Because power dissipation follows the formula $P=I^2R$, increasing operating voltage to the highest practical limit will result in greater output power at a given current (internal power dissipation). Conversely power dissipation can be reduced for a given output power by increasing voltage and reducing current.

Graphs are generally not provided for multiple combinations of current and voltage. Rather the emphasis is on the calculation of power dissipation and thermal resistance, thus enabling the designer to calculate die temperature for the system's combination of voltage, current, and heat sinking.

Shown in Figure 3 is an infrared image of a SA57-IHZ driving a brushed DC motor with a continuous current of 3 A at a supply voltage of 24 V. The numbers mark the local temperatures of the design. The high and low-side FETs of the active half-bridge can clearly be seen as white dots, representing a temperature of approximately 110°C. This picture shows the temperature gradients across the silicon.

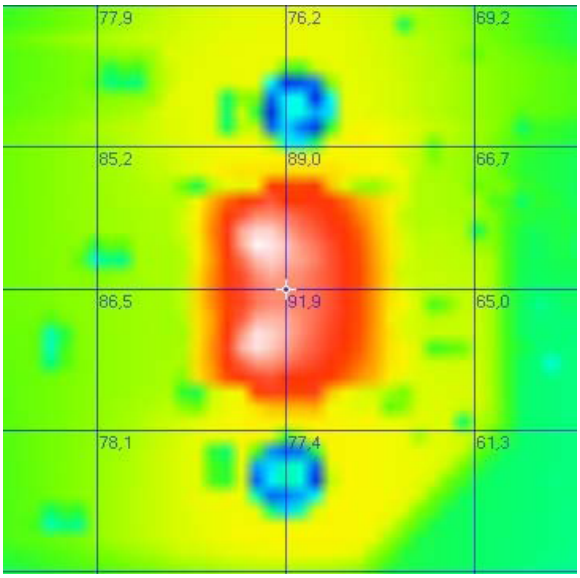

Figure 3. Infrared picture of a SA57 running at 3 amperes at 24 volts.

The heat generated at the two hot-spots spreads over the silicon area. The result is a core temperature of approximately 90°C. The red area represents the heat slug of the IC. This temperature is nearly equal to the core temperature of the silicon. The heat is transferred to the heatsink on the backside (yellow) and in this case to the top and bottom layer (green) of the PCB, then dissipated into the ambient air. (Note that the apparent temperature difference of the screws is the result of emissivity differences between the screws and the rest of the test system. In steady-state operation the screws are approximately the same temperature as the heatsink).

Optimized Motor Commutation Methods

The ON-resistance of the power FETs is the primary contributor to heat generation within a motor drive. In calculating the power lost to the ON resistance we use the standard power formula $P=I^2R$, where I = the current flowing through the motor and R = the ON-resistance of the IC. As the SA57-IHZ and SA306-IHZ offer direct access to each single FET, it is possible to use alternative commutation techniques to increase the system performance and to reduce thermal loads.

The best example for a simple system optimization is sinusoidal commutation of a 3-phase brushless DC motor. This method offers increased efficiency and reduced power dissipation. Alternate types of commutation are more feasible now that virtually every motor control system has some type of micro-controller or DSP/DSC available.

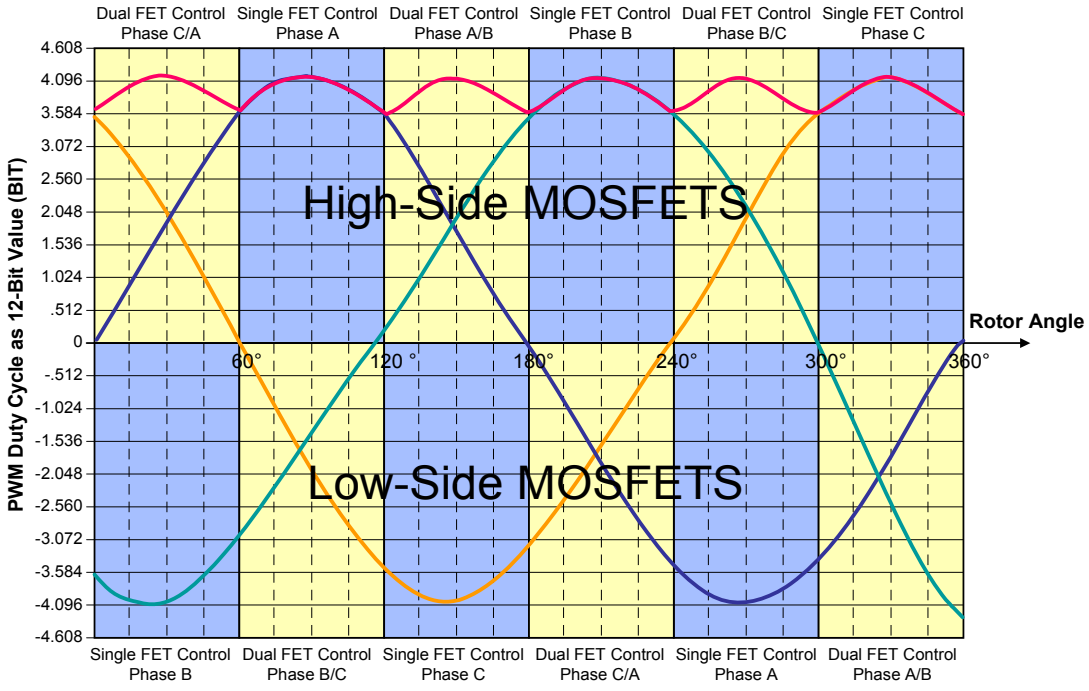

Figure 4. Power and voltage behavior in the case of 3-phase sinusoidal commutation.

Sinusoidal commutation of a 3-phase BLDC motor spreads the generated heat over a wider area of the silicon than with block commutation. This reduces localized heating in the die. During sinusoidal commutation the current through the motor is delivered by two high-side FETs and a single low-side FET or, in the next step, by using a single high-side FET and two low-side FETs. This means that there are always two active FETs in parallel which decreases the ON resistance of the two parallel conducting FETs. The resulting resistance is not linear because the on-time of each PWM signal of the two FETs connected in parallel follows a sinωt/cosωt relation. (See yellow areas in Figure 4)

The effective ON resistance across an electric commutation cycle can be calculated by dividing the ON-resistance value of the parallel high or low side FETs by √2. Using this commutation technique can, in addition to several other advantages, reduce the thermal load by approximately 10% to15%.

The undissipated power can be used to drive the motor or to reduce the total power consumption. In either case the overall efficiency of the system is increased.

Balancing the Electrical Load

As we have just discussed, the main heat generating contributor is the current flowing through the power FETs. Because the SA57-IHZ and the SA306-IHZ are high-voltage devices suitable for supply voltages up to 60 V, an increase in the supply voltage can lead to a decrease of the continuous current for a given power level and therefore to a decrease of the thermal load.

From this point of view, the basic idea is to increase the supply voltage while keeping the continuous current constant to reduce the thermal load. In a pulse-driven system with an inductive load, the relation between voltage and current is not linear so we have to take a closer look at switching losses and the current characteristics under various operation conditions.

An application is balanced when the forward and backward magnetization of the inductor is fully realized within a single PWM cycle. This should be the normal operating condition in applications with constant rotation speed and low dynamics, such as fans, pumps or unidirectional drives. In these applications, once accelerated, the motor runs at a constant speed with a constant mechanical load.

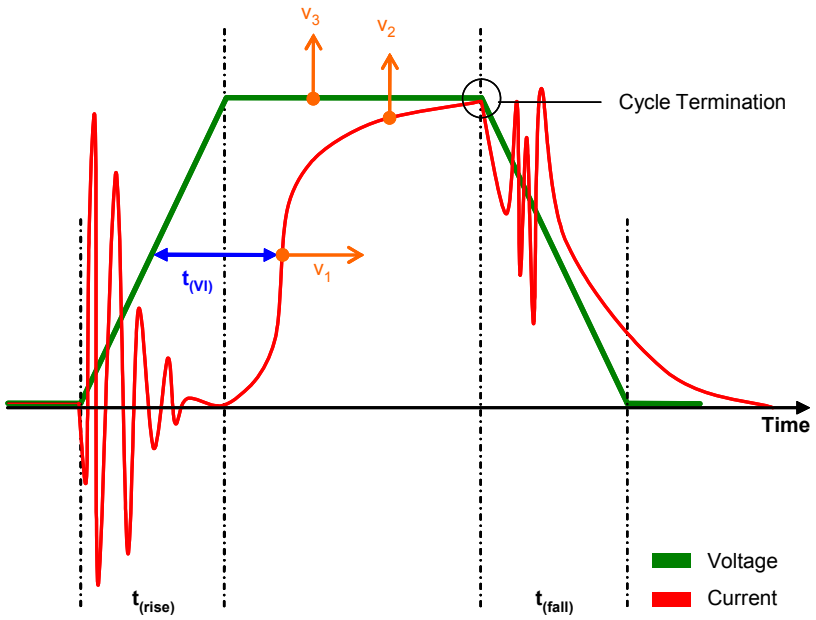

Figure 5: Characteristic of voltage and current during a PWM pulse in a balanced system

Shown in Figure 5 are the characteristics of the voltage and current during a PWM pulse in a balanced operating situation. The rising and falling edges of the voltage are nearly linear within the period given by the time value for the raising and falling edges – typically 200 nanoseconds. The current characteristic depends on the technical parameters of the motor winding. The windings produce a reverse voltage when the rising edge occurs. The current reaches its maximum when the supply voltage and the reverse voltage are more or less equal. The resulting phase shift is represented by t_{VI}. When the supply voltage v_3 is being increased, the phase shift t_{VI} becomes wider as shown by arrow v_1 and the rising edge of the current v_2 appears later. The termination of the duty cycle shuts down the current immediately and always at the same point in time. So when the supply voltage increases, both curves change in the directions indicated by the arrows labeled v_1, and v_2.

Shown in Figures 6 and 7 are voltage and current (overshoot not visible) plots resulting from a PWM pulse applied to phase A. Both 10 V and 30 V supply voltages are shown.

When we look at the falling edge of the PWM pulse, we see that the current drops with the same slew rate at a supply voltage of both 10 V and 30 V, but for a longer time interval because of the higher peak current. This means that the switching losses increase on the falling edge. At the rising edge of the PWM pulse the current is less, so that the switching losses on this side have decreased.

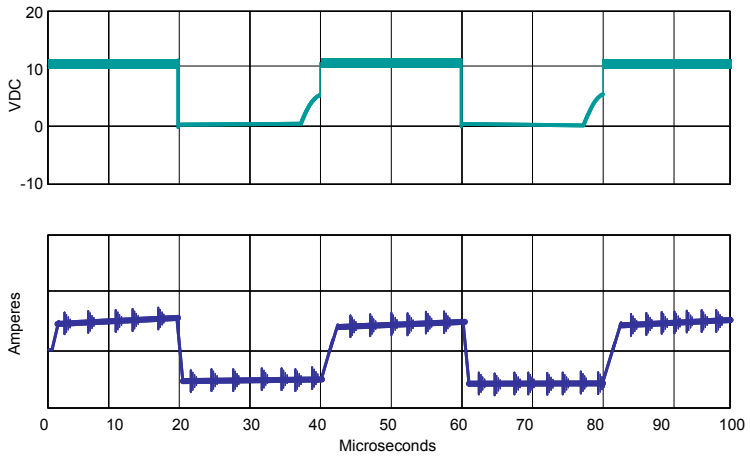

Figure 6. Voltage (green) and current (blue) during a PWM pulse on phase A at a supply voltage of 10 V DC, a 25 kHz switching frequency and a 50% duty cycle.

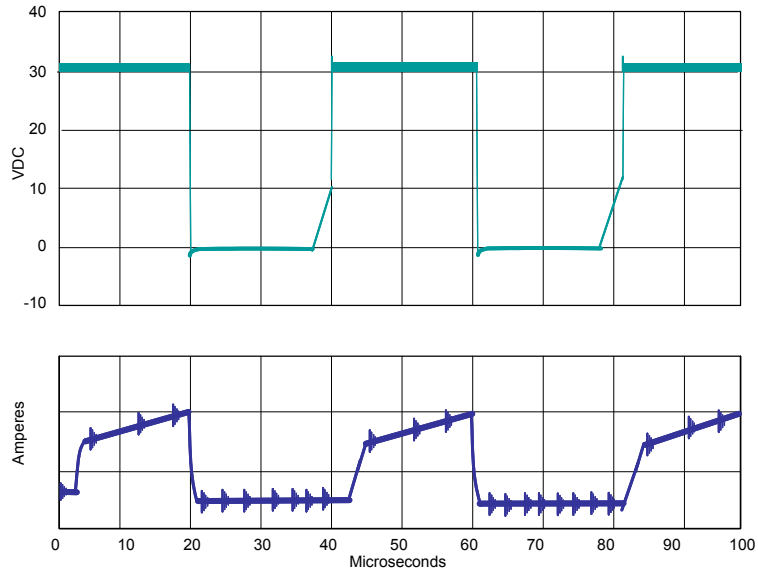

Figure 7. Voltage (green) and current (blue) during a PWM pulse on phase A at a supply voltage of 30 V DC, a 25 kHz switching frequency and a 50% duty cycle.

When we compare the total average current over time, we find similar values at a supply voltage of 10V and 30V. Although the peak current at 30 V is approximately 30% higher, the pulse width is 20% shorter and the slope of the pulse top is steeper than at 10 V. In an overall comparison the average current of both pulses is nearly constant with slightly increased switching losses.

Because the average current remains similar, the average temperature due to I^2R losses within the FETs is also similar. However, because voltage delivered to the motor does increase, there is greater power available to the motor windings. This fact results in increased efficiency by driving motors at higher voltages.

Defining a Movement Profile

In some applications, such as servo drives for positioning or robotics, we find a wide variety of specific operation modes, including periodic acceleration or stalled motor operation with high torque and low rotational speed. In these operating modes the system is not “balanced” since the motor windings are not allowed to achieve complete forward and backward magnetization within a single PWM cycle.

In these conditions the motor windings can become over energized, or saturated with power. As this begins to occur, increased motor current no longer produces proportional increases in torque and increased heating can occur in the FETs of the device. In some cases the motor windings are over energized to obtain the torque required to brake the mechanical load, resulting in a major change of the current waveform characteristic.

In these modes of operation, t_{VI} becomes smaller and a high current peak appears at the raising edge of the PWM pulse as shown in Figure 8. The more the supply voltage v_3 increases the higher the current peak v_2 will be. This current peak can reach multiples of the continuous current.

The plots in Figure 9 depict the relationship between duty cycle, continuous current and temperature at a supply voltage of 20 V DC.

By separating the performance graph in Figure 9 into two parts, the balanced operation (A) and the over energized operation (B) can be better analyzed. During balanced operation, the current and voltage waveforms follow the relationships shown in Figure 5. The phase shift t_{VI} increases so that the continuous current and temperature increase only slightly. When the motor winding starts being over energized (B), t_{VI} decreases rapidly as shown in Figure 8. The current peak at the rising edge of the PWM cycle increases the total average current and the thermal load. Over energized conditions normally happen in the 60-70% duty cycle range. This range corresponds with the knee of the curves in Figure 9. The exact point is dependent on both the quality of the motor and the operating condition. The operating condition with the expected maximal thermal load and its maximal time interval is the basis for the selection of the best mounting technique and heat sinking method.

The 64-pin Power QFP package used for the SA306-IHZ and SA57-IHZ lends itself to different kinds of mounting and heat sinking options which can be used under different operating conditions to realize the best results according to performance and total system cost. In the following sections suggestions are provided on how to select the best solution for your application.

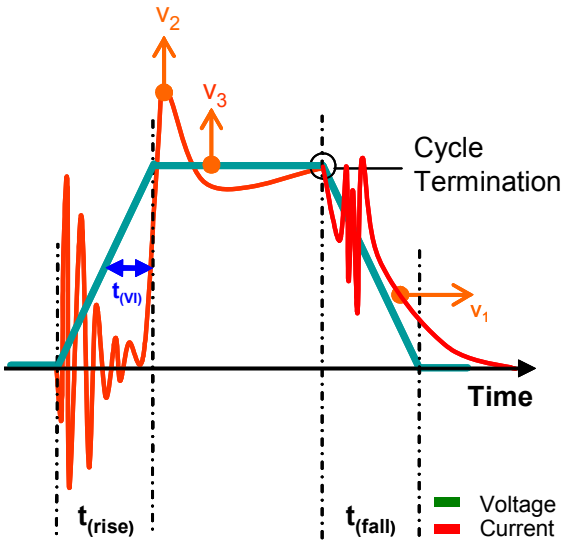

Figure 8. Voltage (green) and current (blue) during a PWM pulse over energizing a motor winding

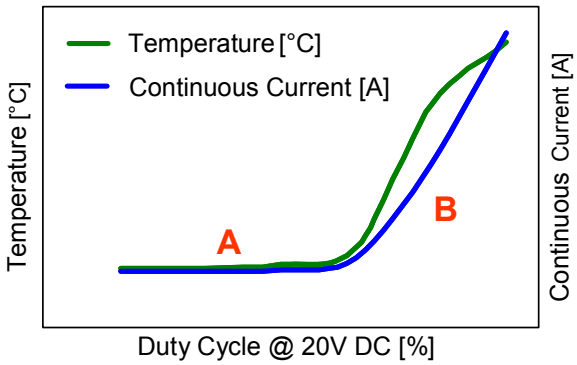

Figure 9. Temperature and continuous current vs. PWM duty cycle during a stalled motor operation

Cooling Options and Results with the 64-pin QFP Package

The size and orientation of the heatsink must be selected to manage the average power dissipation of the driver ICs. Applications vary widely and various thermal techniques are available to match the required performance. This section discusses several techniques that are appropriate for different power levels.

The following examples were developed to evaluate different mounting and cooling options and to define their basic capabilities. Derivation of maximum power and thermal system dynamics is shown in Appendix A.

Two different sets of tests were conducted on the SA306-IHZ. For the first set of tests the power devices were mounted on a PCB with a Digital Signal Controller (DSC). This DSC offers an enhanced motion control interface and allows a designer to commutate the motor in different ways. For the second set of tests a power test bench was used to show the effect of steady state currents on power dissipation and thermal performance.

SMT Mounting without Heatsink in Low-Power Applications

The most cost effective way of mounting either of the SA306-IHZ or SA57-IHZ devices is to solder them directly on a PCB without any further heat sinking components. The heat slug of the 64-pin QFP package offers optimized heat transfer to the PCB (as shown in Figure 10). The IC package, including the heat slug, can be soldered to the top layer of the PCB. Beneath the heat slug, several vias can be used to optimize heat transfer to the backside of the board. The copper area used for the power ground is also used for better thermal coupling to the ambient air.

As part of the tests, semiconductor temperature sensor was placed in the middle of the heat slug area to measure the backside (maximum) heat slug temperature. At an output power of 20 W, a temperature gradient of 99.6°K was obtained. This indicates that the junction temperature will be approximately 130°C at an ambient temperature of 30°C. The plots in Figure 11 denote a value of 136°C at an ambient temperature of 27°C with a total thermal resistance for the system of approximately 5.343 K/W.

Using the thermal resistance value, the maximum output power can be calculated for an application covering the industrial temperature range up to +85°C at approximately 9 W. This result is valid for static operation under the specific set of voltage and current conditions. In applications with frequent accelerations and decelerations it is important to know the thermal response time. This value provides an indication for the time required to transfer a specific amount of heat from the die to the backside of the board. Derivations for calculating thermal resistance and maximum power dissipation can be found in Appendix A. Shown in Figure 12 is the temperature characteristic of the ground plane from the ambient to the maximum temperature when the motor is driven continuously at an output power of 9 W.

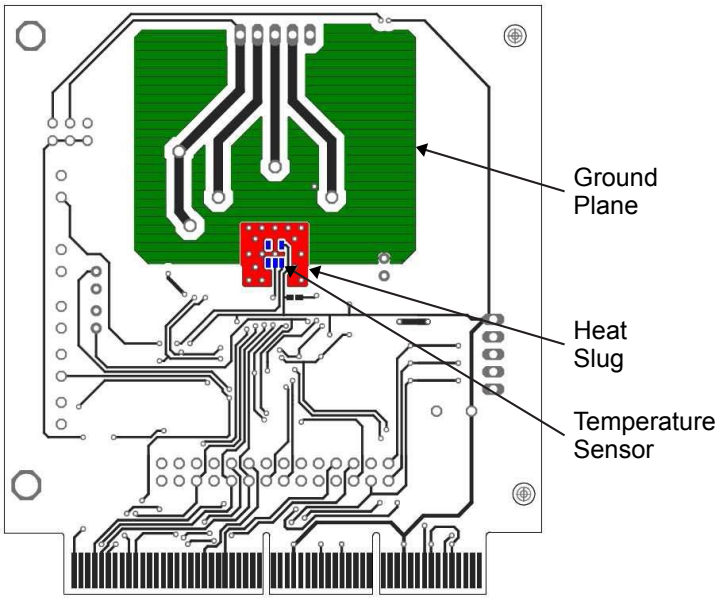

Figure 10. Bottom layer of the PICtail™ plus test board for low power applications

Conclusion

Although the maximum output power rating of 8 W to 9 W seems low, these devices are still capable of delivering PEAK currents up to 15 A for several seconds. In addition, increased voltage or reduced ambient temperature may result in increased power capability. This makes the SA57-IHZ and SA306-IHZ unusually well suited for applications using gears with high transmission rates where large mechanical loads have to be accelerated through start-up phase and end at high speeds with lower power requirements.

This mounting technique is appropriate for smaller, low-power or high-speed drives in cost sensitive applications such as fans, pumps, scanners, surveillance cameras, labeling machines or paper feeders – all where size and production costs are crucial.

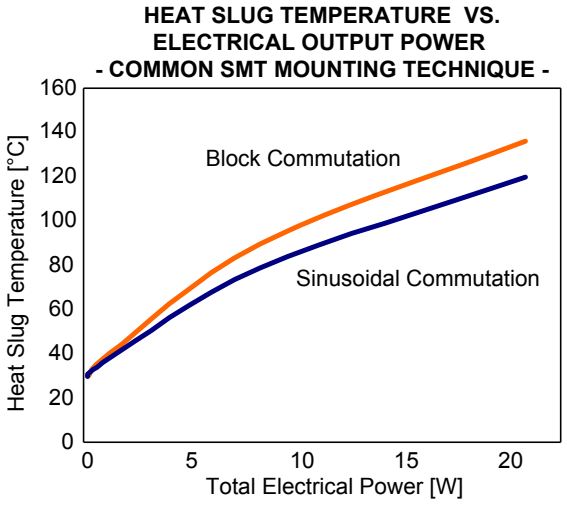

Figure 11. Temperature characteristic of the SA306-IHZ mounted on test board for low-power applications

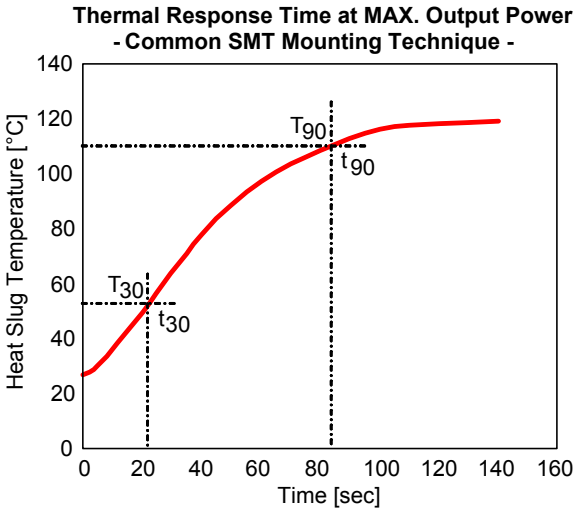

Figure 12. Thermal response time at MAX output power of 9 W

SMT Mounting with Thermal Pad and Heatsink for Mid-Range Power Applications

For applications where higher output power is required for a longer period of time, but ease of production is still a main design issue, an additional test board was designed where the SA306-IHZ is still mounted in the conventional manner. However, beneath the IC is a 100mm² cut out. A thermal pad is used to transfer the heat from the heat slug directly to the HS33 heatsink.

The thermal pad is made from a polymer that contains materials chosen for low thermal resistance, such as silver. These pads remain soft for years and therefore can accommodate any shifting that may occur to equalize between materials

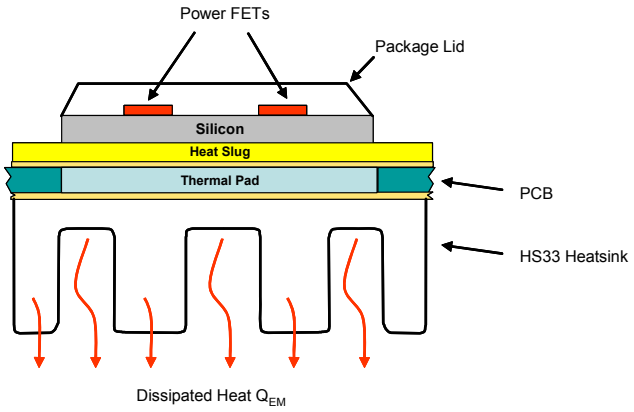

Figure 13. Simplified cross sectional view of the thermal system of the mid-power test board

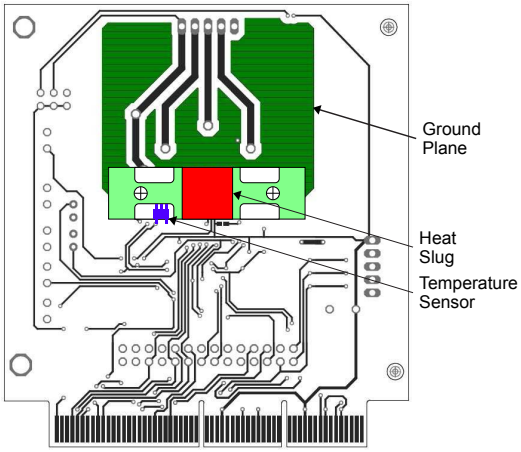

Figure 14. Bottom layer of the test board for mid-range power applications

with different coefficients of expansion that is likely to occur due to temperature changes. On the mid-power test board a 2mm thermal pad is used to fill the gap between the heat slug and the heatsink (see Figure 13). The thermal pad chosen is a Berquist™ Gap Pad 5000S35.The cutout area is 10mm x 10mm.

This board design provides three advantages:

- The SA306-IHZ is still mounted like a conventional SMT part, including the side-wings of the heat slug.
- Thermal coupling is always constant, even if the thickness of the PCBs varies from 1.5mm to 1.7mm.
- Accurate placement of the heatsink is not required.

Shown in Figure 14 is the back of the mid-power test board. The 100mm² heat slug area (red) has been cut out to accommodate the thermal pad. The temperature sensor has been moved to a natural cut out of the HS33 heatsink. The height of the sensor package is exactly the height of the cut out. The thermal coupling comes about due to the intimate contact of the package top with the heatsink.
The heatsink is mounted with two screws. Note that the light green area of the heatsink has direct contact with the dark-green ground plane area. With this mounting technique the total thermal resistance is reduced while the contact area is increased to ambient air. Although the HS33 heatsink is used on this test board, it is not essential. A thermal pad could also be used to couple the heat slug to the enclosure to improve the thermal path. The 100mm² x 1.5mm thick thermal pad with its thermal conductivity of 86 W/mK has a thermal resistance of 0.174 K/W. When this value is compared to the

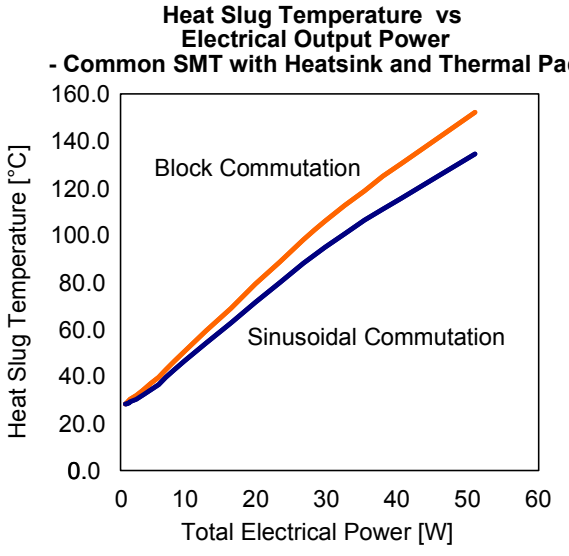

Figure 15. Temperature characteristic of the SA306-IHZ mounted on the test board for mid-range power applications using a thermal pad and the HS33 heatsink

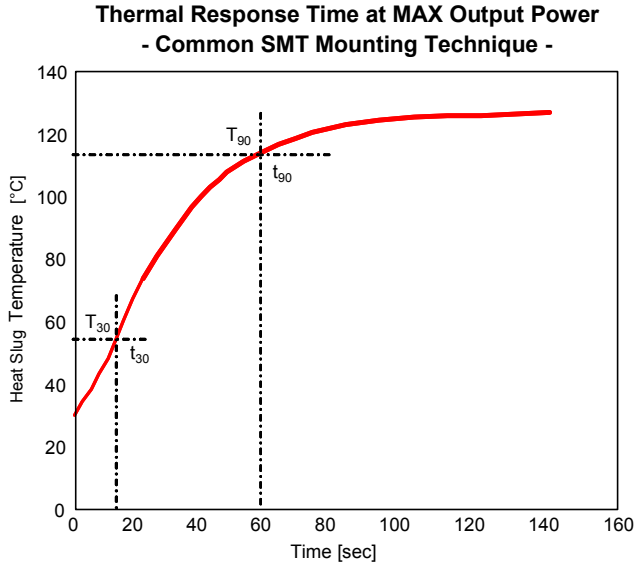

Figure 16. Thermal response time at output power of 20 W

previous model with vias, this solution provides less than a 10th of the thermal resistance.

Using the thermal pad, approximately 51 W of continuous output power is achieved with die temperatures of approximately +155°C at an ambient temperature of +26°C using block commutation. The maximum power output, up to +85°C for this configuration is approximately 20 W at the chosen voltage and current. With this solution it is possible to double the output power at similar system temperatures. What is most important is the improved performance over the short heat path to the heatsink due in part to the low thermal resistance through the thermal pad.

Conclusion

The thermal pad offers easy system assembly and good thermal performance at moderate power ratings. The short thermal path affords benefits in accelerating heavy mechanical loads for a longer time. This is an appropriate solution for a wide variety of industrial applications using gears and with production runs in mid-range volumes.

Flipped-Over SMT Mounting with Heatsink for High-Power Applications

The third test board uses the same heat sinking method as the Apex Microtechnology Evaluation Boards DB63R and DB64R. This technique is also described in the *High-Power Heatsinking* section.

This time the SA306-IHZ is flipped over and mounted. The heatsink is then mounted directly onto the heat slug of the IC. This shortens the thermal path from the IC to the ambient air and reduces the total thermal resistance of the system to a minimum of 1.674 K/W.

Shown in Figure 17 is the assembly of the IC and heatsink on the test board for high-power applications. The position of the temperature sensor, the mounting method of the heatsink and the thermal coupling to the ground plane are still the same. The only difference is that the SA306-IHZ is flipped over and soldered in a precise cutout from the backside of the board. A picture of the actual mounting technique can be seen in Figure 20.

As a result of this mounting technique, the characteristics of the temperatures in Figure 18 become quite linear across the whole power range. The output power at a die temperature of 135°C is approximately 52 W at +25°C and approximately 29 W at +85°C. This solution provides only a slightly higher maximum output power than the thermal pad. However, the short thermal path has its advantages in dynamic applications. The fast response time between the die and the heat slug provides benefits in applications where multiple accelerations occur over short time spans (see Figure 19).

Conclusion

The principal advantage of the flipped-over mounting is that it provides a short heat path for supporting high dynamic applications. The free access to the heat slug offers a wide variety of heat sinking methods and more effective cooling options.

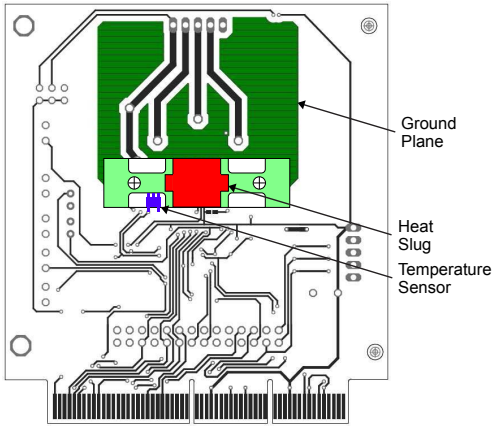

Figure 17. Bottom layer of the test board for high-power applications

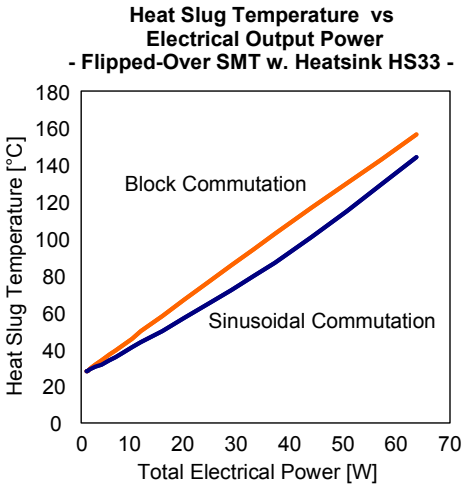

Figure 18. Temperature characteristic of the SA306-IHZ mounted flipped over on the test board for high power applications using the HS33 heatsink

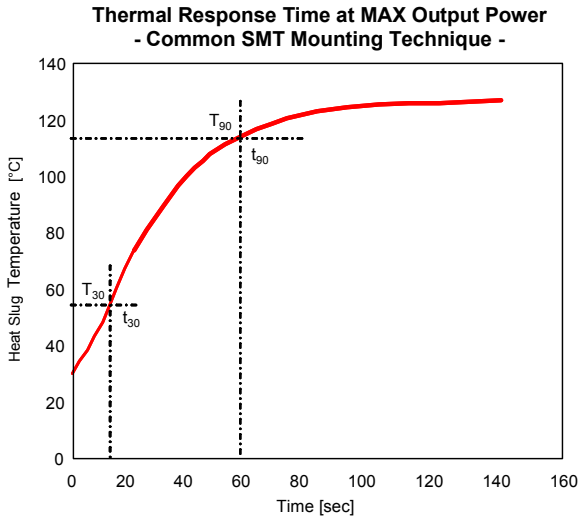

Figure 19. Thermal response time at a output power of 25 W

Comparisons of the Low-Power, Mid-Range Power and High-Power Test Board

The following table compares the benchmark values for each mounting technique in a side-by-side comparison. Please note that the columns for the maximum output power are rated for ambient temperatures of +25°C and +85°C. There is a more detailed chart for the power dissipation derating across ambient temperatures in the *Power Dissipation Derating* section.

Table 1. Temperature characteristics of the SA306-IHZ mounted flipped over on the PICtail™ Plus test board for high-power applications using the HS33 heatsink

Mounting Technique	Calculated MAX Output Power @ +85°C (W)	MAX Output Power at Test Voltage @ +25°C (W)	MAX Continuous Current at Test Voltage @ +25°C (A)	Total Thermal Resistance R_{TH} (K/W)	Average Thermal Response Time k90(K/sec)
Common SMT	9.0	19	0.93	2.789-5.343	1.323
Common SMT with Pad & Heatsink	19.8	38	2.73	0.628-2.529	1.869
Flipped Over with Heatsink	23.9	52	4.12	0.801-1.726	2.637

All values in this Section are the result of actual tests under laboratory conditions and should provide an indication of the capabilities of several design variants. The behavior of these ICs may differ under different design and operation conditions.

High-Power Heat Sinking

Since the SA306-IHZ is designed for higher power applications, it is also necessary to determine heat sinking factors that allow for higher power dissipation. Because of the concentration of heat as a result of power density, it is important to use heatsink types that provide short thermal paths. For this reason large extrusions with fins on wide centers have not been included in this evaluation.

Dissipation capacity with two types of aluminum extrusions were evaluated. The HS33 is a small heatsink, 0.4" x 0.4" x 1.5", that has four fins on 0.118-inch centers. This configuration places all four fins directly under the heat slug of the SA306-IHZ package. The HS33 heatsink is shown in Figure 20. This heatsink is used on the Apex Microtechnology DB64R evaluation board for the SA306-IHZ.

The second heatsink in Figure 21 is a pin configuration with dimensions of 1" x 2" x 2". The pins are 0.070" in diameter on 0.137" centers. This highly effective heatsink provides multiple heat paths directly under the silicon. Because of its size, it is capable of safely dissipating much higher power levels than the HS33.

The test set-up for the HS33 used the Apex Microtechnology DB64R evaluation board with an 8Ω resistive load. To increase power, the DC voltage across the board and load were increased. This set-up does not fully simulate the operation of a motor. However, it does allow stable temperatures to be achieved, thus facilitating measurement. This set-up met the goal of allowing power dissipation and die temperature measurements with varying heatsinks.

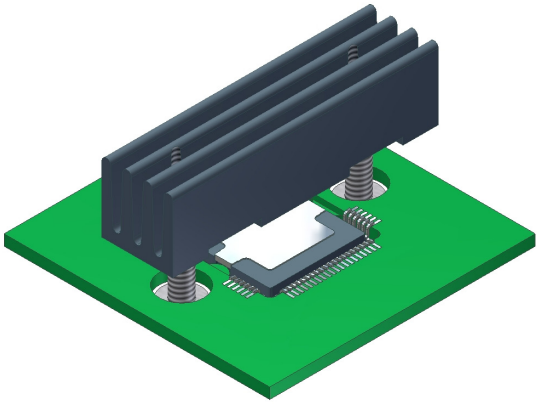

Figure 20. HS33 Finned Heatsink with SA306-IHZ

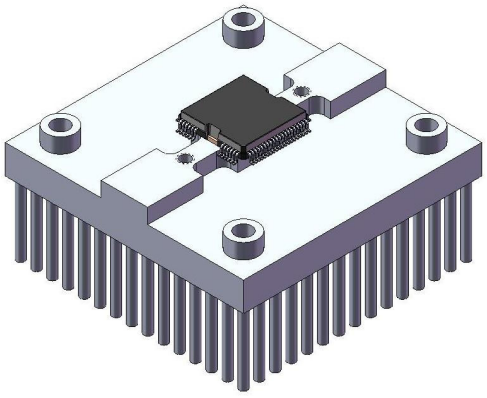

Figure 21. Pin Heatsink with SA306-IHZ

Table 2. Results of Thermal Testing

Configuration	Orientation	Convection	Dissipated Power (W)	Output Power @ 85% Efficiency (W)	Heatsink Temp MAX (ºC)	Junction Temp MAX (ºC)	Thermal Resistance (ºC/W)
HS33 and PCB	Horizontal, HS down	Natural	7.5	42.5	139	145	16
HS33 and PCB	Vertical, HS vertical	Natural	9	51	138	146	13
HS33 and PCB	Horizontal, HS down	Forced	17	96.3	127	140	6.8
Pin Heatsink	Horizontal, HS up	Natural	16	90.7	125	141	7.3
Pin Heatsink	Horizontal, HS down	Forced	39	221.0	79	113	2.3

Five different thermal configurations were tested, and the results are shown in Table 2. Note that consistent with real world applications, the differences in test set-up and measurement techniques between this test and the previous section produce different test results and power capabilities. This is to be expected and shows that designers must take into account their specific operating environment when evaluating thermal performance.

Three rows of HS33 data are shown in Table 2. The first two used convection cooling only. As one might assume, placing the heatsink in a horizontal position does not produce as effective a cooling surface as placing the heatsink vertically. With a vertical heatsink under convection conditions the heatsink dissipates 9 W, allowing 50 W of motor power at a +140°C junction temperature. Thermal resistance results with the vertical heatsink measured 13°C/W junction to air.

The third HS33 test was performed using a small fan blowing across the board. The object was to simulate an enclosed housing with a fan providing outside air, similar to a PC. In this case, dissipation improved to 17 W and allowing almost 100 W at the motor at 85% efficiency. Thermal resistance junction-to-case also improved dramatically to 6.8°C/W.

Subsequent testing with this configuration suggests that use of a small fan, in this case a 1" Sunon unit (PN GM0502PFV1-8, similar to MPU or graphics chip FAN), directed onto the HS33, allows heatsink dissipation in excess of 21 W and suggesting motor power of approximately 120 W. Under these conditions, die temperature should not exceed +140°C.

For full-power applications, the pin heatsink was tested. The pin heatsink was tested under both convection and forced-air conditions. The test board and fan can be seen in Figure 22. The fan used was a 2" Sunon (PN KDE1205PHV2) capable of 595 linear feet per minute of air flow. The retaining screws for the fan also hold the heatsink and the device in place on the board. The test configuration for the pin heatsink used a modified PCB layout and a 4Ω resistive load.

Under normal convection conditions, this heatsink was able to dissipate 16 W of power, allowing motor power of 91 W, similar to the HS33 with airflow. However, when using forced air with this heatsink, power dissipation within the heatsink increased to almost 40 W, allowing for greater than 220 W of power to the motor. In addition, the junction temperature dropped to +113°C, suggesting this is a high reliability configuration with room for increased power output. The junction to air thermal resistance also improved dramatically, measuring 2.3°C/W. With some increase in die temperature and a well designed system, the pin heatsink in a forced air configuration will allow the full 48 W and 5 A rating of the device.

Use of a heatsink does increase system cost. In some cases, the designer may find that a small amount of airflow across an HS33-type heatsink provides sufficient dissipation and lower costs versus a larger heatsink. However, for full power dissipation, use of a large heatsink with forced air may be necessary.

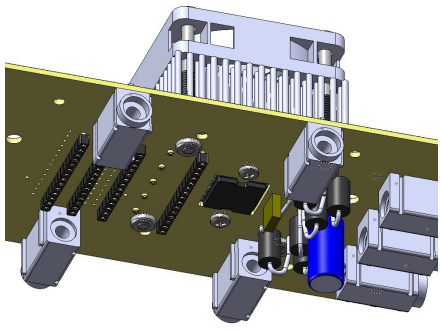

Figure 22. Pin heatsink and test board with fan attached

Power Dissipation Derating

To provide high-reliability operation, the die temperature must be kept to a safe level. The designer must consider total power, heatsink capability and ambient temperature in order to make appropriate system choices. The graph in Figure 23 shows derating curves for power. Curves are given for load power versus heatsink and ambient temperatures. In addition, curves are given for single-sided and double layer PCBs.

Figure 23 also shows that below +25°C the SA306-IHZ can operate above 300 W, assuming die temperatures are held to a reliable level. Above +30°C improved heat sinking must be employed or the device may need to be derated. Again, actual power capability is a function of operating voltage, efficiency, ambient temperature and heatsink capability. Actual derating will vary based on these factors. It should also be noted that the derating of heatsinks themselves change with temperature and therefore with power dissipation. As shown in Figure 24 for the HS33, both airflow and ambient temperature play a role in accurately modeling the dissipation capability of the heatsink.

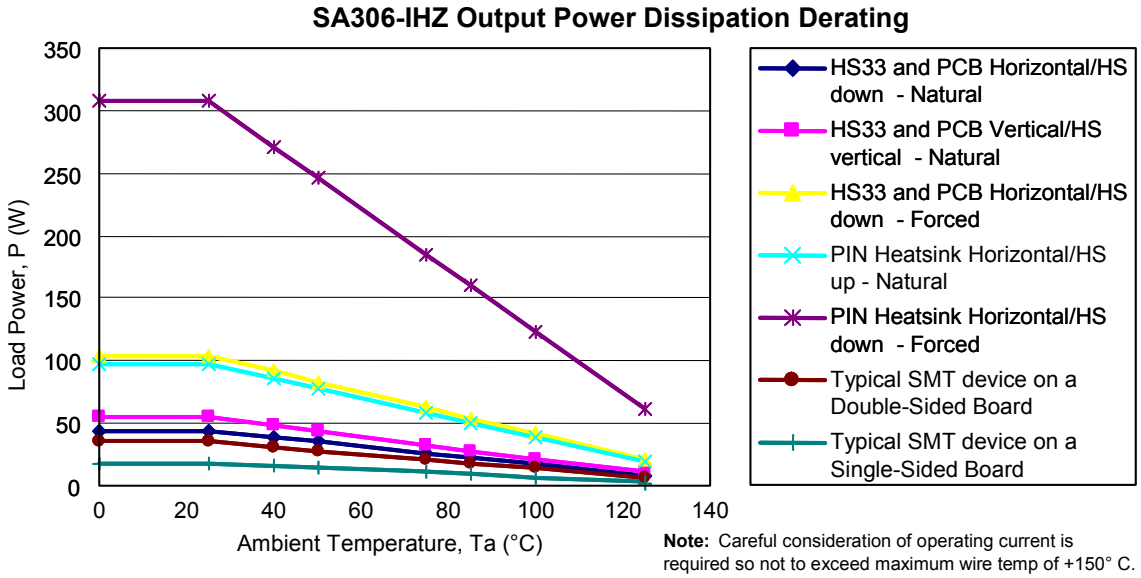

Figure 23. Load power derating curves for ambient temperature, Ta (°C)

Conclusion

Applications vary widely and various thermal techniques are available to match the required performance. The size and orientation of the heatsink must be selected to manage the average power dissipation of the IC. Standard PCB mounting techniques enable these devices to dissipate as much as 9 W. The use of a heat pad or the patent-pending mounting technique shown in Figure 20, with the SA306-IHZ inverted and suspended through a cutout in the PCB, is adequate for power dissipation exceeding 20 W.

In free air, mounting the PCB perpendicular to the ground, so that the heated air flows upward along the channels of the fins, can provide improved cooling. In applications in which higher power dissipation or lower junction or case temperatures are required, a larger heatsink or circulated air can significantly improve performance. A pin heatsink can successfully dissipate the thermal energy generated when driving motors in excess of 200 W. By using the techniques in this Application Note, the SA57-IHZ and SA306-IHZ can provide long-term, reliable motor control in a very compact package.

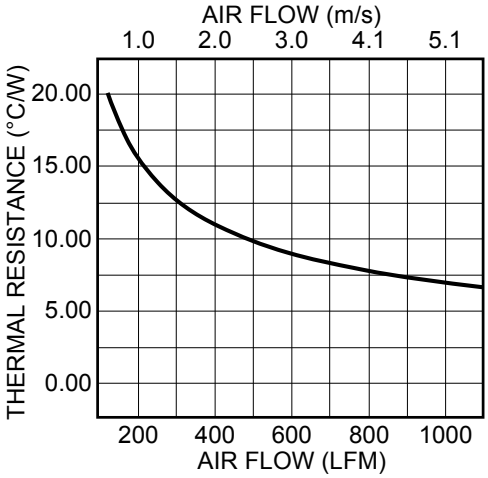

Figure 24. Heatsink thermal resistance versus air flow

References

1. *SA57-IHZ Pulse Width Modulation Amplifier* Data Sheet, www.apexanalog.com
2. *SA306-IHZ Pulse Width Modulation Amplifier* Data Sheet, www.apexanalog.com
3. *3-Phase Switching Amplifier* Application Note SA306-IHZ, AN46, www.apexanalog.com

Appendix A – Derivation of Maximum Power and Thermal Dynamics Values for PCB Based Tests

Section A.1 Result for Common SMT Mounting with Heatsink in Low-Power Applications

The total thermal resistance of the common SMT model for a SA306-IHZ is 4.98 K/W (Kelvin per watt). To calculate the maximum output power for this mounting technique without specific values for voltage or current, we have to transform the equation:

$$T_0 - T_2 = \left(\frac{1}{\alpha A} + R_{th}\right) \bullet R_{DS(ON)} \bullet I_C^2$$

$$T_0 - T_2 = \left(\frac{1}{\alpha A} + R_{th}\right) \bullet P_E \quad (12)$$

Where:

T_0 = SA306-IHZ or SA57-IHZ junction temperature
T_2 = ambient air temperature
P_E = electrical output power

The plots in Figure 7 denote a value of +136°C at an ambient temperature of +27°C with a thermal resistance of approximately 5.343 K/W. The difference is due to the fact that the factor includes the thermal resistance into the ambient air and is therefore a combined value for $(\alpha A)^{-1} + R_{th}$.
When we use the value for the thermal resistance of the PICtail™ Plus Test Board to calculate the maximum output power for an application covering the whole industrial ambient temperature range up to +85°C, the maximum continuous output power is approximately 9 W:

$$P_{MAX} = \frac{T_0 - T_2}{R_t}$$

$$P_{MAX} = \frac{135°C - 85°C}{5.343\ \frac{K}{W}} = 9.4W \quad (13)$$

Where:

T_0 = SA306-IHZ orSA57-IHZ junction temperature
T_2 = ambient air temperature
R_T = total thermal conductivity
P_{MAX} = MAX electrical output power

Shown in Figure 12 is the temperature characteristic of the ground plane from the ambient to the maximum temperature, when the motor is driven continuously at a maximum power of 9 W. For later comparisons the focus is on the transfer ratio $\Delta T_{30}/\Delta t_{30}$ and $\Delta T_{90}/\Delta t_{90}$, described by a quotient K for the slew rate from the cold state to 30% and 90%, respectively, of the maximum temperature.
The slew rate quotient *k* is an indication for the quality of the dynamic behaviour of the thermal system:

$$k = \frac{\Delta\theta}{\Delta t} = \frac{T_1 - T_0}{t_1 - t_0}$$

$$k_{30} = \frac{54.5°C - 26.8°C}{21\ sec} = 1.317\ \frac{K}{sec} \quad (14a)$$

$$k_{90} = \frac{109.7°C - 26.8°C}{84\ sec} = 0.988\ \frac{K}{sec} \quad (14b)$$

Where:

k = slew rate quotient in Kelvin per second
Δθ = temperature difference in Kelvin
Δt = duration in seconds
T_0= temperature at time t_0
T_1 = temperature at time t_1

Section A.2 SMT Mounting with a Thermal Pad and Heatsink for Mid-Range Power Applications

The first order approximation of the thermal model gives a thermal resistance of 2.678 K/W. The following equation is used to verify the real value of the complete system:

$$T_0 - T_2 = \left(\frac{1}{\alpha A} + R_{th}\right) \bullet P_E$$

$$\frac{T_0 - T_2}{P_E} = \left(\frac{1}{\alpha A} + R_{th}\right)$$

$$R_t = \frac{155°C - 26°C}{51W} = 2.529\ \frac{K}{W} \quad (15)$$

Where:
T_0= SA306-IHZ or SA57-IHZ junction temperature
T_2 = ambient air temperature
P_E = electrical output power
R_t = total thermal conductivity

Next is to find the maximum power rating to cover the total industrial range for ambient temperatures up to +85°C at a maximum die temperature of +135°C.

$$P_{MAX} = \frac{T_0 - T_2}{R_t}$$

$$P_{MAX} = \frac{135°C - 85°C}{2.529\ \frac{K}{W}} = 19.8W \quad (16)$$

Where:
T_0 = SA306-IHZ or SA57-IHZ junction temperature
T_2 = ambient air temperature
R_t = total thermal conductivity
P_{MAX} = Max. electrical output power

The chart in Figure 12 shows the improvements of the thermal dynamics. The slew rate quotients k_{30} and k_{90} are:

$$k = \frac{\Delta\theta}{\Delta t} = \frac{T_1 - T_0}{t_1 - t_0}$$

$$k_{30} = \frac{55.8°C - 26.8°C}{15\ sec} = 1.938\ \frac{K}{sec} \quad (17a)$$

$$k_{90} = \frac{114.7°C - 26.8°C}{63\ sec} = 1.407\ \frac{K}{sec} \quad (17b)$$

Where:
k = slew rate quotient in K/s
Δθ = temperature difference in Kelvin
Δt = duration in seconds
T_0 = temperature at time t_0
T_1 = temperature at time t_1

Section A.3 Flipped Over SMT Mounting with Heatsink for High-Power Applications

The following equations are used to calculate the estimated maximum output power for ambient temperatures of +85°C:

$$\frac{T_0 - T_2}{P_E} = \left(\frac{1}{\alpha A} + R_{th}\right)$$

$$R_t = \frac{135°C - 26°C}{52W} = 2.096\ \frac{K}{W}$$

$$P_{MAX} = \frac{T_0 - T_2}{R_t}$$

$$P_{MAX} = \frac{135°C - 85°C}{2.096\ \frac{K}{W}} = 28.97W \quad (18)$$

Where:
T_0 = SA306-IHZ/SA57-IHZ junction temperature
T_2 = ambient air temperature
R_t = total thermal conductivity
P_{MAX} = MAX electrical output power

Using this mounting technique, the following values are obtained for k_{30} and k_{90}:

$$k = \frac{\Delta\theta}{\Delta t} = \frac{T_1 - T_0}{t_1 - t_0}$$

$$k_{30} = \frac{58.5°C - 26.8°C}{12\ sec} = 2.638\ \frac{K}{sec} \quad (19a)$$

$$k_{90} = \frac{121.8°C - 26.8°C}{53\ sec} = 1.792\ \frac{K}{sec} \quad (19b)$$

Where:
k = slew rate quotient in K/s
Δθ = temperature difference in Kelvin
Δt = duration in seconds
T_0 = temperature at time t_0
T_1 = temperature at time t_1